



EXPERIMENTAL INVESTIGATION OF THE EFFECTS OF WATER ADDITION INTO THE INTAKE AIR ON COMBUSTION PARAMETERS, ENERGY BALANCE AND DEVELOPING AN EMPIRICAL COMBUSTION DURATION RELATION IN AUTOMOBILE DIESEL ENGINE

Mustafa TUTI*, Zehra ŞAHİN** and Orhan DURGUN***

*Karadeniz Technical University, Faculty of Marine Science, Naval Architecture and Marine Eng., Trabzon, mtuti@ktu.edu.tr, ORCID: 0000-0002-2309-3735

**Karadeniz Technical University, Faculty of Engineering, Mechanical Engineering Dep., Trabzon, zshahin@ktu.edu.tr, ORCID: 0000-0002-7140-2061

***Avrasya University, Faculty of Engineering and Architecture, Mechanical Engineering Dep., Trabzon, odurgun@ktu.edu.tr, ORCID: 0000-0001-6381-0690

(Geliş Tarihi: 14.03.2023, Kabul Tarihi: 25.10.2023)

Abstract: The effect of the water addition into the intake air (WAIA) on cylinder pressure, temperature, heat release rate (HRR), combustion duration (CD), and energy balance in an automotive diesel engine have been investigated experimentally. Also, an empirical correlation has been developed for estimating CD using the HRR. This relation has been developed by applying the multiple curve fitting method, taking into account experimental results for different water ratios such as (2, 4, 6, 8, and 10) %, different engine loads, and different engine speeds such as (2000, 2500, 3000, 3500, and 4000) rpms. The test results showed that cylinder pressure values generally increased at (2000, 2500, and 3500) rpm, but they decreased at (3000 and 4000) rpm for all of the selected water ratios. Also, maximum cylinder temperature values have occurred at crank angles farther from TDC for WAIA. Cylinder temperature values mostly decreased at (2000, 2500, and 3000) rpms, but they generally increased at (3500 and 4000) rpms for WAIA. Also, maximum cylinder temperature values were occurred at crank angles farther from TDC for WAIA. HRR values generally decreased at (2000, 2500, 3500, and 4000) rpms, but they generally increased at 3000 rpm. It has been determined that the CDs were generally shortened at all of the engine speeds under full loads with water addition. CD values for NDF and (2.42, 4.22, 5.95, 8.32, 9.46) % water ratios have been determined as (13.10, 12.96, 12.93, 12.68, 12.95, and 13.576) °CA, respectively, at 2000 rpm. The effective power values according to the chemical energy of the fuel generally decrease with WAIA at 2000 rpm. However, the effective power values according to the chemical energy of the fuel increase for high WRs at 4000 rpm.

Keywords: Diesel engines, Water addition into the intake air, Heat release rate, Combustion duration, Energy balance

BİR OTOMOBİL DİZEL MOTORUNDA EMME HAVASINA SU EKLENMESİNİN YANMA PARAMETRELERİ VE ENERJİ DENGESİ ÜZERİNDEKİ ETKİLERİNİN DENEYSEL İNCELENMESİ VE YANMA SÜRESİ İÇİN AMPİRİK BAĞINTI GELİŞTİRME

Özet: Sunulan çalışmada; bir otomobil dizel motorunda emme havasına su eklenmesinin (EHSE) silindir basıncı, silindir sıcaklığı, açığa çıkan ısı oranı değerleri, enerji dengesi ve yanma süresi üzerindeki etkileri deneysel olarak incelenmiştir. Ayrıca, açığa çıkan ısı oranı eğrilerinden hesaplanan yanma süreleri için çoklu eğri uydurma yöntemi kullanılarak ampirik bir bağıntı geliştirilmiştir. Bu bağıntı geliştirilirken, farklı yükler altında (2000, 2500, 3000, 3500 ve 4000) d/d devir sayılarında ve % (2, 4, 6, 8, ve 10) su oranlarında yapılan deneysel veriler kullanılmıştır. Yapılan çalışma sonunda, EHSE'nin silindir basınçlarını (2000, 2500 ve 3500) d/d devir sayılarında artırdığı ve (3000 ve 4000) d/d devir sayılarında azalttığı ve maksimum basınçların üst ölü noktaya (ÜÖN'ye) daha yakın krank mili açılarında (KMA) oluştuğu belirlenmiştir. EHSE'nin silindir sıcaklıklarını (2000, 2500 ve 3000) d/d devir sayılarında azalttığı ve (3500 ve 4000) d/d devir sayılarında artırdığı ve maksimum sıcaklıkların ÜÖN'ye daha yakın krank mili açılarında oluştuğu görülmüştür. EHSE ile açığa çıkan ısı oranı değerleri (2000, 2500, 3500 ve 4000) d/d sayılarında azalmış, ancak 3000 d/d devir sayısında artmıştır. EHSE ile, yanma süresi tam yük altında seçilen tüm çalışma koşullarında genel olarak azalmıştır. Örneğin 2000 d/d devir sayısında, saf dizel yakıtı ve % (2.42, 4.22, 5.95, 8.32, 9.46) su oranlarında yanma süreleri (13.10, 12.96, 12.93, 12.68, 12.95, and 13.576) KMA şeklinde hesaplanmıştır.

EHSE ile, motorda harcanan yakıtın kimyasal enerjisine göre değerlendirme yapıldığında efektif gücün 2000 d/d devir sayısında genellikle azaldığı ancak 4000 d/d devir sayısında arttığı belirlenmiştir.

Anahtar kelimeler: Dizel motorları, Emme havasına su eklenmesi, Açığa çıkan ısı oranı, Yanma süresi, Enerji dengesi

NOMENCLATURE

CA	Crank angle
HRR	Heat release rate [J/deg.]
n	Engine speed [rpm]
NDF	Neat diesel fuel
TDC	Top dead center
T _b	Brake torque
WAIA	Water addition into the intake air
WR	Water ratio
CD	Combustion duration [°CA]

INTRODUCTION

Diesel engines, known as the most efficient thermal machines, face two kinds of challenges: the crisis of petroleum and the increasingly stringent emission regulations (Gzahal, 2009). For this reason, scientists and engine manufacturers work intensively on structural and alternative fuel developments related to diesel engines to minimize these undesired effects. Clean combustion strategies, high-pressure fuel injection systems such as common-rail, the new developments in valve and control systems, and, turbocharging etc., can be listed as some examples of these structural studies. The use of different alternative fuels to replace fossil fuels in diesel engines can be given as examples of alternative fuel developments. Biodiesel and bioethanol are among the most studied alternative fuels in this context (Maawa et al., 2020; Han et al., 2020). In addition, water adding method in diesel engines has gained importance in recent years as the use of water significantly reduces NO_x, which is the most crucial pollutant of diesel combustion (Subramanian, 2011; Şahin et al., 2018; Tauzia et al., 2010). As well known from relevant literature; water use allows for controlling combustion temperature, which affects NO_x production (Gzahal, 2009).

Since the 1950s, many different studies have been carried out on the addition of water in diesel engines (Mahmood et al., 2019). Nowadays, the number of studies on the addition of water in diesel engines has increased due to the rising environmental pollution and depletion of crude oil resources. It can be seen from the literature review that, although many different techniques for water adding have been used in diesel engines, generally, three methods were applied. These methods can be classified as (a) water/diesel emulsion, (b) water injection directly into the cylinder (DWI) using a separate injector, and (c) water addition/injection into the intake air (WAIA) (Maawa et al., 2000; Şahin et al., 2018; Shojoei et al., 2019; Ayhan and Ece, 2020).

(a) Water/diesel emulsion method is applied by blending and homogenizing diesel fuel and water (here, a suitable surfactant is generally added to this mixture). This water/surfactant/diesel fuel mixture is injected into the cylinder using the conventional injection system at the end of the compression stroke. This technique

requires almost no modification to the engine. Zhu et al. (2019) summarized the disadvantages of this method as follows: (1) One of the main disadvantages of this method is the limitation of the amount of using water that can be added to fuel. (2) An excess of water may be injected into the cylinder either too early or too late in the combustion process in this method, which results in the cooling of the entire cylinder and lead to increased ignition delay, engine noise, and retarded combustion. (3) This method may cause problems at low loads, for example, at the initial operating conditions of the diesel engine. These disadvantages may limit the use of water/diesel emulsion technique in vehicle diesel engines. However, there are many studies in the literature applying this method (Gowrishankar et al., 2020; Jhalani et al., 2019; El Shenawy et al., 2019). Besides these studies, water emulsification has also been applied with different alternative fuels (Maawa et al., 2020; Khanjani and Soboti, 2021; Elsanusi et al., 2017) in recent years. For example, when biodiesel is used in diesel engines, it increases NO_x emissions compared to diesel fuel because biodiesel contains oxygen. For this reason, it is desired to prevent the increase of NO_x emissions by applying biodiesel/diesel fuel blends with water emulsion recently (Maawa et al., 2020; Elsanusi et al., 2017). Maawa et al. (2020) carried out an experimental study by using conventional diesel fuel, blended biodiesel 20% (B20), and B20 emulsified with three different water ratios. They determined that the emulsification of biodiesel/diesel with water decrease effectively exhaust emissions, especially NO_x emissions, with no penalty in engine performance. In this study, the B20 with emulsified 30% water reduced the NO_x emissions by approximately 26.17% compared to diesel fuel. Elsanousi et al. (2017) investigated the effects of biodiesel/diesel fuel blends with different ratios of water emulsion on engine performance and exhaust emissions in a light-duty diesel engine. In this study, diesel fuel and two different canola oil biodiesel (20, 40 % vol.) /diesel fuel blends were emulsified with three different water ratios such as 5%, 10%, and 15%. They reported that as the increasing water content in emulsion fuel, BTF increases and NO_x and smoke emissions decrease significantly. However, emulsion fuel containing a higher water increase considerably CO emissions. There are a lot of similar studies in the literature (Maawa et al., 2020; Khanjani and Soboti, 2021; Elsanusi et al., 2017). In these studies, the effects of water/diesel fuel emulsions (or water/diesel fuel/different alternative fuel emulsions) on engine performance and exhaust emissions were investigated.

(b) Water injection directly into the cylinder using a separate injector. In this technique, the water amount and distribution in the cylinder can be controlled at the appropriate time. However, this method is expensive and difficult to apply (Gowrishankar et al., 2020). Hence, there is a limited number of researches about this method in the literature (Ayhan and Ece, 2020; Sun et al., 2022; Zhang et al., 2017). Zhang et al. (2017)

studied the effects of DWI during compression stroke on the indicated thermal efficiency optimization in a common-rail diesel engine. They found that the application of this method increases indicated thermal efficiency by up to 4.08 %. A similar study was carried out on a marine diesel engine based on the three-dimensional simulation model by Sun et al. (2022). In this study, the effect of DWI at the compression stroke on engine performance and NO_x emissions was investigated. They found that for the W/F ratio is 2.0, the indicated power and NO_x emissions decrease 3.2% and 55.6%, respectively.

(c) WAIA is also applied using an adapted carburetor or a low-pressure injector. This method can be easily and economically realised. In addition to these advantages of WAIA method, it can increase the volumetric efficiency, and it forms a more homogeneous water/air mixture distribution in the combustion chamber, too (Subramanian, 2011; Gowrishankar et al., 2020). In this method, although the injection time of water is not changed, the injection time of diesel fuel can be adjusted to obtain optimum operating conditions. In the literature, there are also various studies applying this method (Subramanian, 2011; Şahin et al. 2018). Subramanian (2011) experimentally compared the effects of water/diesel emulsion and water injection into intake air (WAIA) on the combustion, performance, and emission characteristics of a DI diesel engine under similar operating conditions. The water-diesel ratio for both methods was selected as 0.4:1 by mass. He found that water/diesel fuel emulsion and WAIA drastically reduce NO_x and smoke emissions. In this study, he reported that the water emulsion in reducing smoke and NO_x levels is more effective than WI. However, it was determined that CO and HC levels of water emulsion were higher than WAIA. Water injection into the intake air method was applied for biodiesel (Tesfa et al., 2012). Tesfa et al. (2012) experimentally investigated water injection into intake air (WAIA) in a four-cylinder, direct injection (DI) turbocharged diesel engine running with pure biodiesel. The results indicated that WAIA at a rate of 3 kg/h results in a 50% decrease in NO_x emissions without causing any significant alteration in the specific fuel consumption. Also, it was observed that WAIA has little effect on cylinder pressure and heat release rate.

There are a lot of studies investigating the effects of the above-mentioned methods on diesel engine performance characteristics, combustion, and exhaust emissions. From these researches, it can be seen that the water adding in diesel engines reduces NO_x and smoke emissions simultaneously without any considerable fuel penalty (Subramanian, 2011; Şahin et al., 2018). However, there are few studies on the effects of water adding on combustion characteristics and CD. For these reasons, in the present study, the effects of WAIA on combustion characteristics and duration have been experimentally investigated in an automotive diesel engine. Also, an empirical correlation has been developed for estimating CD using the HRR curves,

which were determined from measured cylinder pressure values. This relation has been developed by applying the multiple curve fitting method, taking into account experimental results for different water ratios such as (2, 4, 6, 8, and 10) %, different engine loads, and different engine speeds such as (2000, 2500, 3000, 3500, and 4000) rpms. As these experiments were carried out in an automotive diesel engine currently used in motor vehicles is very important for providing new information to the industry. In addition, energy balance was investigated at 2000 and 4000 rpms under full load for different water ratios in this study.

MATERIALS AND METHODS

Engine and Experimental Set-up

Neat diesel fuel (NDF) and water adding tests were conducted in a current turbocharged-automotive diesel engine. Table 1 shows the main technical specifications of this engine and Figure 1 presents a schematic view of the test system. A water brake was used for loading the engine, and the brake moment was electronically measured. Cylinder gas pressure was measured by using an AVL GH13P type quartz pressure sensor without cooling. The main specifications of this sensor are given in Table 2.

Experimental Study

In the present study, tests were carried out at (2000, 2500, 3000, 3500, and 4000) rpms engine speeds and for approximately (2, 4, 6, 8, and 10 %, by vol.) WRs under six different loads. However, only full load results have been given in the present paper. Firstly, NDF tests were conducted as NDF values were required for comparing water addition results. After NDF tests were completed, the adapted carburetor was mounted on the intake manifold of the engine. Figure 1 presents the technical view of the adapted carburetor. Information about the adapted carburetor was given in the authors' previous studies (Şahin et al. 2018; Şahin et al. 2014). In addition, to introduce water into the intake air and to measure the amount of the added water, a small water tank, a scaled glass bulb, and a flexible pipe were used and this water adding unit is shown in Figure 1. Any other modification on the experimental system and engine was not done. The main steps of the experiments are briefly given in the following paragraph.

Table 1. Technical specifications of the engine.

Engine	Renault K9K 700 turbocharged-automotive diesel engine
Displacement	1.461 liter
Cylinder number	4
Bore & stroke	76 & 80.5 mm
Compression ratio	18.25: 1
Maximum power	48 kW @ 4000 rpm
Maximum torque	160 Nm @ 1750 rpm
Connecting rod length	130 mm
Injection system	Common rail injection system*
Nozzle hole numbers and	5 and 0.12 mm

diameter	
----------	--

*The injection pressures up to 2000 bar

Table. 2. Main specifications of the pressure transducer

Sensor type and model	Piezoelectric (GH13P)
Measuring range [bar]	0-150
Sensitivity [pC/bar]	15.25
Natural frequency [kHz]	115
Linearity	< ±0.3 %

The test engine was run for nearly (20-30) minutes before the tests, and when the cooling water temperature reached the level of (70 ±5) °C, that is steady-state conditions were reached, NDF and various WRs experiments were performed. For example, at 2000 rpm, firstly, the engine load was adjusted to 150 Nm. Then, the mean jet opening of the carburetor was adjusted to the 1st opening, which gives ~2 % WR. After ~2 % WR tests were carried out for loading moments between (150-75) Nm by reducing the engine load at 15 Nm steps and simultaneously adjusting the gas throttle position suitably to obtain a constant 2000 rpm. Thus, ~2 % WR tests under six different engine loads were performed. After that, for obtaining ~4 % WR, the main jet opening of the carburetor was adjusted to the 2nd opening, and this opening was again retained and fixed at the same 2000 rpm. Thus, tests for ~4 % WR were carried out under the above-selected six different engine loads. Then, the similar experimental procedure for approximately (~6 %, ~8 %, and ~12 %) WRs at 2000 rpm was performed. The similar tests were performed for the same loads and WRs at (2500, 3000, 3500, and 4000) rpms.

Energy Balance Calculation

The energy balance calculation in the used test engine is divided into the control volume as shown in Figure 1b. Here, the energy items entering the control volume were the enthalpy of the intake air, $Q_{in,a}$; the energy of turbocharged system, W_K ; the fuel chemical energy, Q_f ; and energy of water added to the intake air, Q_{H_2O} . The energy items leaving the control volume were the effective power, N_e ; energy loss during the exhaust gas flow, Q_{exh} ; the heat transfer rate to the cooling fluids, Q_w ; energy spent on all of the unaccounted heat losses, Q_{ol} . Thus, the energy balance formula is written as follows.

$$Q_{in,a} + Q_f + Q_{H_2O} + W_K = N_e + Q_{exh} + Q_w + Q_{ol} \quad (1)$$

$$Q_{ol} \text{ (kW)} = (Q_{in,a} + Q_f + Q_{H_2O} + W_K) - (N_e + Q_{exh} + Q_w)$$

In relation 1, $Q_{in,a}$ is the energy of the enthalpy of the intake air at the intake temperature. This value has been ignored since the range in intake air temperature is small. Q_f is the fuel chemical energy, Q_{H_2O} is the energy of water added to the intake air, and W_K is the

compression work of the compressor. These values were computed as follows.

$$Q_f \text{ (kW)} = \frac{B_t \cdot H_{LHV}}{3600} \quad (1a)$$

$$Q_{H_2O} \text{ (kW)} = \frac{\dot{m}_{H_2O} \cdot H_{H_2O}}{\mu_{H_2O}} \quad (1b)$$

where, B_t (kg/h) is the total fuel consumption, H_{LHV} (kJ/kg) is the lower heating values of the fuel, \dot{m}_{H_2O} (kg/s) is the flow rate of water addition to the intake air. H_{H_2O} (kJ/kmol) is the formation enthalpy of water and μ_{H_2O} is the molecular mass of water. B_t was calculated as follows.

$$B_t \left(\frac{\text{kg}}{\text{h}} \right) = \frac{m_f \cdot 3600}{1000 \cdot \Delta t} \quad (1c)$$

Here, m_f is the mass of consumed diesel fuel during Δt (s), and here it was taken as 30 g. The amount of the water consumed during this time interval (m_{H_2O}) was determined by using a scaled glass bulb as can be seen in Figure 1a.

$$W_K \text{ (kW)} = 0.6 W_T \quad (1d)$$

where W_T is the turbine work and calculated as follows:

$$W_T \text{ (kW)} = \dot{m}_{exh} (c_{p,Tout} T_{T_{out}} - c_{p,Tin} T_{T_{in}}) \quad (1e)$$

where \dot{m}_{exh} is the flow rate of exhaust gases, and in this study \dot{m}_{exh} is calculated as $\dot{m}_{exh} = (\dot{m}_f + \dot{m}_a + \dot{m}_{H_2O})$. In relation 1e, $c_{p,Tin}$ is the specific heat capacity of exhaust gases at $T_{T_{in}}$ (K) the inlet exhaust gases temperature to the turbine and $c_{p,Tout}$ is the specific heat capacity of exhaust gases at $T_{T_{out}}$ (K) the outlet exhaust gases temperature from the turbine, respectively.

$$N_e \text{ (kW)} = 0.1013 \frac{T_b \cdot \omega}{P_0} \sqrt{\frac{T_0 \cdot X_{hum}}{293}} \quad (1f)$$

$$\dot{Q}_{exh} \text{ (kW)} = \frac{(\dot{m}_{exh} \cdot c_{p,exh} \cdot (T_{exh} - T_0))}{3600} \quad (1g)$$

$$\dot{Q}_{cw} \text{ (kW)} = \frac{\dot{m}_{cw} \cdot c_{p,cw} \cdot (T_{out} - T_{in})}{60} \quad (1h)$$

In formula 1e, T_b (Nm) is the torque, was measured in the test system. T_0 (K) is the ambient temperature and P_0 (MPa) is the ambient pressure. These values were measured in the experiment. X_{hum} is the humidity correction which is determined depending on dry and wet thermometer temperatures. In formula 1f, $c_{p,exh}$ (kJ/kgK) is the specific heat capacity of the exhaust gas at T_{exh} (K) exhaust temperature. In relation 1g, \dot{m}_{CW} (kg/h) is the flow rate of cooling water, $c_{p,cw}$ (kJ/kgK) represent the specific heat capacity, T_{in} (K) and T_{out} (K) are the inlet and outlet temperature of cooling water.

Heat Release Rate (HRR) Analysis

In this paper, using the following relationship, HRR values has been calculated (Heywood, 1988).

$$\frac{dQ}{d\theta} = \frac{\gamma}{\gamma-1} P \frac{dV}{d\theta} + \frac{1}{\gamma-1} V \frac{dP}{d\theta} \quad (2)$$

where $dQ/d\theta$ (J/deg.) is the heat release rate, γ is the specific heats ratio, V (cm³) is the cylinder volume, and P (bar) is cylinder pressure. Here, HRR analysis has been conducted along the crank angle steps during the time interval of inlet valve closure and exhaust valve opening. The mean cylinder temperature values were calculated from the ideal gas equation. The specific heat ratio values were calculated at selected crank angles depending on the temperature values, computed from the ideal gas equation.

Deriving of Quadratic Empirical Relation for CD

The heat release rate (HRR) curves, which were calculated from measured pressure values, were shown in Figures (2a, 3a, 4a, 5a, and 6a) and these values have been used to determine the CDs. That is, in the present study, HRR values have been determined by using measured cylinder pressures and corresponding volume values. Then, HRR curves have been drawn for NDF and five different WRs under various loads at (2000, 2500, 3000, 3500, and 4000) rpms. Thus, every one of the CDs was determined separately for operating conditions by using these HRR curves.

Here, CD is defined as the time interval between crank angles corresponding to 10% and 90% values of HRR (Shojoei et al., 2019; Boldaji et al., 2018; Singh et al., 2015). Finally, an empirical relation for the CD, which takes into account the effects of water rate, the loading level and the engine speed, is developed. Here a multiple variable quadratic curve-fitting method was applied to the experimental CD values which were originally developed by Durgun and Kafali (1991). Naturally, the load ranges for the used speeds are different from each other, as shown in Table 3. The same load values must be used to develop the empirical relation for the burning duration. For this reason, identical selected load values are marked in yellow colour in Table 3, and these values are used in curve fitting computations. CD values, determined from HRR curves, for selected engine speeds and WRs under (120, 105, 90, and 75) Nm loads are shown in Table 4, Table 5 and Table 6, respectively. Using the CD values under (120, 105, 90, and 75) Nm loads, an empirical relation has been developed depending on the water ratio (WR), load value (L) and the number of revolutions (n).

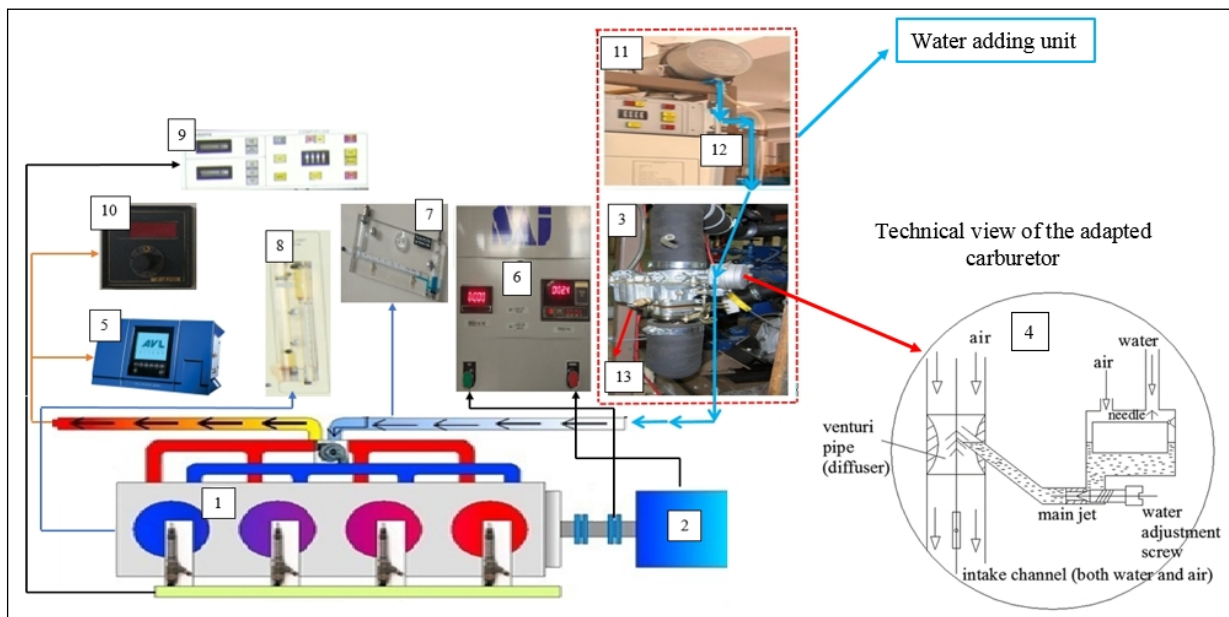


Figure 1a. Schematic view of the experimental setup. 1-Diesel engine, 2-hydraulic dynamometer, 3-carburator, 4-detailed drawing of the carburetor, 5-gas analyzer, 6-load measurement indicator, 7-inclined manometer, 8-coolont flow meter, 9-fuel measurement unit, 10-digital display for temperatures, 11-water tank, 12-scaled glass bulb, 13-water adjustment screw

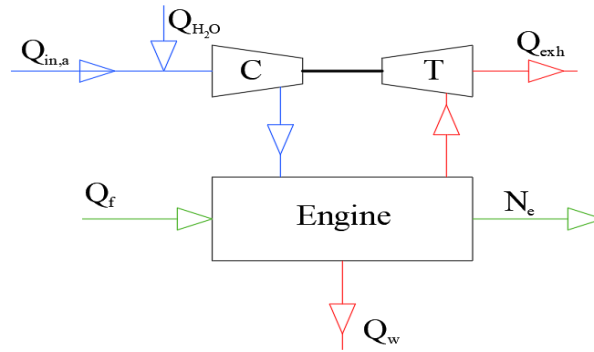


Figure 1b. Schematic of the energy balance of the used test engine. The abbreviations in this figure: C and T are shown as compressor and turbine, respectively.

Here, CD (°CA) is the combustion duration, WR (%) is the water ratio, n (rpm) is the engine number of revolutions, and L (Nm) is the load value.

Table 3. Selected load values corresponding to the various engine speeds

Speed (rpm)	150 Nm	135 Nm	120 Nm	105 Nm	90 Nm	75 Nm	60 Nm	45 Nm
2000	X	X	X	X	X	X	-	-
2500	X	X	X	X	X	X	-	-
3000	-	X	X	X	X	X	X	-
3500	-	-	X	X	X	X	X	X
4000	-	-	X	X	X	X	X	X

In this way, the effects of three parameters, such as n, WR, and, L were taken into account in the empirical CD formula. Here, as explained in the above paragraph, multiple regression was applied to the experimental data to develop the CD relation. However, here, the multiple regression was carried out in the form of nested loops, which is easier.

The aimed empirical CD formula can be a function of the water ratio, engine speed and load value as follows:

$$CD = f(WR, n, L) \quad (3)$$

The calculation process of this multiple curve fitting method consists of the following steps:

Step 1: While applying this method, firstly, the engine speed and the load were taken as constant. Thus, for the CD, a quadratic curve was fitted depending on the water ratio values for every situation. In this way, a quadratic relation is obtained for CD as follows:

$$CD = a_0 \cdot (WR)^0 + a_1 \cdot (WR)^1 + a_2 \cdot (WR)^2 \quad (4)$$

Using the CD data at (2000, 2500, 3000, 3500, and 4000) rpms under selected loads (120, 105, 90, 75) Nm given in Tables 4-8, the following relations are obtained.

Table 4. The determined CD values for 5 different WRs at 5 different engine speeds under 120 Nm

WR (%)	2000 rpm	2500 rpm	3000 rpm	3500 rpm	4000 rpm
NDF	12.798	21.077	20.752	21.300	24.858
2	12.648	21.221	21.177	21.022	24.02
4	12.941	21.431	21.017	21.254	24.921
6	12.507	20.823	21.243	21.579	24.641
8	12.647	20.848	20.314	21.611	24.942
10	12.841	21.033	20.088	21.611	24.560

Table 5. The determined CD values for 5 different WRs at 5 different engine speeds under 105 Nm

WR (%)	2000 rpm	2500 rpm	3000 rpm	3500 rpm	4000 rpm
NDF	17.301	21.980	25.488	20.526	22.462
2	17.760	21.972	25.263	20.526	22.200
4	16.416	21.830	25.505	20.044	21.618
6	17.752	21.972	25.053	20.571	21.900
8	17.021	21.727	25.457	20.263	22.219
10	17.697	21.983	25.553	20.338	22.463

Table 6. The determined CD values for 5 different WRs at 5 different engine speeds under 90 Nm

WR (%)	2000 rpm	2500 rpm	3000 rpm	3500 rpm	4000 rpm
NDF	20.477	22.778	25.698	23.369	20.417
2	20.059	22.747	25.425	23.107	20.134
4	20.175	22.524	25.698	23.141	20.117
6	20.451	22.699	25.568	22.945	19.832
8	20.318	21.911	25.505	22.681	20.100
10	20.454	22.382	25.521	23.369	20.417

Table 7. The determined CD values for 5 different WRs at

5 different engine speeds under 75 Nm

75 Nm	2000 rpm	2500 rpm	3000 rpm	3500 rpm	4000 rpm
WR (%)	CD (°CA)	CD (°CA)	CD (°CA)	CD (°CA)	CD (°CA)
NDF	21.663	23.310	25.006	25.996	18.900
2	20.393	23.087	25.006	25.055	18.029
4	21.070	23.523	25.022	25.545	18.015
6	20.769	23.097	25.232	25.976	18.012
8	21.265	23.274	25.473	25.489	18.616
10	20.945	23.323	25.085	25.789	19.100

Following equations can be written for $n_1, n_2, n_3, n_4,$ and n_5 ;

$$n_1 = 2000, CD_1 = a_{0,1} + a_{1,1} \cdot (WR) + a_{2,1} \cdot (WR)^2 \quad (5)$$

$$n_2 = 2500, CD_2 = a_{0,2} + a_{1,2} \cdot (WR) + a_{2,2} \cdot (WR)^2 \quad (6)$$

$$n_3 = 3000, CD_3 = a_{0,3} + a_{1,3} \cdot (WR) + a_{2,3} \cdot (WR)^2 \quad (7)$$

$$n_4 = 3500, CD_4 = a_{0,4} + a_{1,4} \cdot (WR) + a_{2,4} \cdot (WR)^2 \quad (8)$$

$$n_5 = 4000, CD_5 = a_{0,5} + a_{1,5} \cdot (WR) + a_{2,5} \cdot (WR)^2 \quad (9)$$

After obtaining CD_1, CD_2, CD_3, CD_4 and CD_5 , it has been passed to the calculation step 2.

Step 2: Quadratic curves were fitted to coefficients (a_0, a_1, a_2) in equations 5-9 depending on the engine speed as given in Eqs. 10-12.

$$a_0 = b_0 + b_1 \cdot n + b_2 \cdot n^2 \quad (10)$$

$$a_1 = c_0 + c_1 \cdot n + c_2 \cdot n^2 \quad (11)$$

$$a_2 = d_0 + d_1 \cdot n + d_2 \cdot n^2 \quad (12)$$

These relations were written in Table 8 according to the selected loads for each engine speed. Thus, the coefficients of the relations (13-24) have been calculated. Then, it has been passed to step 3.

Step 3: As can be seen in Table 9, quadratic curves were fitted to the coefficients ($b_{0,120}, b_{0,105}, b_{0,90}, b_{0,75}, \dots, d_{2,120}, d_{2,105}, d_{2,90}, d_{2,75}$), in relations (13-24), depending on the engine loads.

Table 8. The quadratic curve equations for $a_0, a_1,$ and a_2 for each engine speed under four different loads

L=120 Nm	Relation number	L=105 Nm	Relation number
$a_{0,120} = b_{0,120} + b_{1,120} \cdot n + b_{2,120} \cdot n^2$	(13)	$a_{0,105} = b_{0,105} + b_{1,105} \cdot n + b_{2,105} \cdot n^2$	(16)
$a_{1,120} = c_{0,120} + c_{1,120} \cdot n + c_{2,120} \cdot n^2$	(14)	$a_{1,105} = c_{0,105} + c_{1,105} \cdot n + c_{2,105} \cdot n^2$	(17)
$a_{2,120} = d_{0,120} + d_{1,120} \cdot n + d_{2,120} \cdot n^2$	(15)	$a_{2,105} = d_{0,105} + d_{1,105} \cdot n + d_{2,105} \cdot n^2$	(18)
L=90 Nm		L=75 Nm	
$a_{0,90} = b_{0,90} + b_{1,90} \cdot n + b_{2,90} \cdot n^2$	(19)	$a_{0,75} = b_{0,75} + b_{1,75} \cdot n + b_{2,75} \cdot n^2$	(22)
$a_{1,90} = c_{0,90} + c_{1,90} \cdot n + c_{2,90} \cdot n^2$	(20)	$a_{1,75} = c_{0,75} + c_{1,75} \cdot n + c_{2,75} \cdot n^2$	(23)
$a_{2,90} = d_{0,90} + d_{1,90} \cdot n + d_{2,90} \cdot n^2$	(21)	$a_{2,75} = d_{0,75} + d_{1,75} \cdot n + d_{2,75} \cdot n^2$	(24)

Table 9. The quadratic curves for the the coefficients ($b_{0,120}, b_{0,105}, b_{0,90}, b_{0,75}, \dots, d_{2,120}, d_{2,105}, d_{2,90}, d_{2,75}$), in relations (13-24), depending on the engine loads

b	c	d
$b_0 = e_0 + e_1 \cdot L + e_2 \cdot L^2$ (25)	$c_0 = h_0 + h_1 \cdot L + h_2 \cdot L^2$ (28)	$d_0 = t_0 + t_1 \cdot L + t_2 \cdot L^2$ (31)
$b_1 = f_0 + f_1 \cdot L + f_2 \cdot L^2$ (26)	$c_1 = p_0 + p_1 \cdot L + p_2 \cdot L^2$ (29)	$d_1 = u_0 + u_1 \cdot L + u_2 \cdot L^2$ (32)
$b_2 = g_0 + g_1 \cdot L + g_2 \cdot L^2$ (27)	$c_2 = s_0 + s_1 \cdot L + s_2 \cdot L^2$ (30)	$d_2 = v_0 + v_1 \cdot L + v_2 \cdot L^2$ (33)

At the end, by writing the coefficients (b_0, b_1, \dots, d_2) (25-33) in the equation (3), the following empirical formula for CD has been arranged as follows:

$$CD = A \cdot (WR)^0 + B \cdot (WR)^1 + C \cdot (WR)^2 \quad (34)$$

where A, B, and C have been given in Table 10. A program has been prepared in MATLAB to calculate the

coefficients (A, B, and C) in the relation (34) by using experimentally determined CD values at different engine speeds and WRs under (120, 105, 90, and 75) Nm load conditions. The numerical values of the A, B, and C coefficients of the relation (34) are given in Table 10. The mean absolute percent error (MAPE) of the CD was determined as 5.18% for relation (34).

Table 10. Relations for A, B, and C coefficients in relation 34 and the numerical values of these coefficients

$A = \left\{ \begin{array}{l} [e_0 + e_1 \cdot L + e_2 \cdot L^2] + \\ [f_0 + f_1 \cdot L + f_2 \cdot L^2] \cdot n + \\ [g_0 + g_1 \cdot L + g_2 \cdot L^2] \cdot n^2 \end{array} \right\} \quad (34a)$	$B = \left\{ \begin{array}{l} [h_0 + h_1 \cdot L + h_2 \cdot L^2] + \\ [p_0 + p_1 \cdot L + p_2 \cdot L^2] \cdot n + \\ [s_0 + s_1 \cdot L + s_2 \cdot L^2] \cdot n^2 \end{array} \right\} \quad (34b)$	$C = \left\{ \begin{array}{l} [t_0 + t_1 \cdot L + t_2 \cdot L^2] + \\ [u_0 + u_1 \cdot L + u_2 \cdot L^2] \cdot n + \\ [v_0 + v_1 \cdot L + v_2 \cdot L^2] \cdot n^2 \end{array} \right\} \quad (34c)$
$A = \left\{ \begin{array}{l} [-64.63 + 0.90 \cdot L - 0.004 \cdot L^2] + \\ [0.04 - 6.42 \cdot 10^{-5} \cdot L - 8.69 \cdot 10^{-7} \cdot L^2] \cdot n + \\ [-4.47 \cdot 10^{-6} - 5.35 \cdot 10^{-8} \cdot L + 5.73 \cdot 10^{-10} \cdot L^2] \cdot n^2 \end{array} \right\}$	$B = \left\{ \begin{array}{l} [-27.78 + 0.53 \cdot L - 0.003 \cdot L^2] + \\ [0.02 - 3.80 \cdot 10^{-4} \cdot L + 1.86 \cdot 10^{-6} \cdot L^2] \cdot n + \\ [-3.24 \cdot 10^{-6} + 6.11 \cdot 10^{-8} \cdot L - 2.96 \cdot 10^{-10} \cdot L^2] \cdot n^2 \end{array} \right\}$	$C = \left\{ \begin{array}{l} [2.47 - 0.05 \cdot L + 2.33 \cdot 10^{-4} \cdot L^2] + \\ [-0.002 + 3.47 \cdot 10^{-5} \cdot L - 1.72 \cdot 10^{-7} \cdot L^2] \cdot n + \\ [3.04 \cdot 10^{-7} - 5.76 \cdot 10^{-9} \cdot L + 2.83 \cdot 10^{-11} \cdot L^2] \cdot n^2 \end{array} \right\}$

RESULTS AND DISCUSSION

The Effects of WAIA on Cylinder Pressure, Temperature, HRR and CD

In this section, the effects of WAIA on the cylinder pressure, cylinder temperature, and HRR are presented in Figures 2-6 and evaluated for (2000, 2500, 3000, 3500, and 4000) rpms under only full load conditions for brevity. These figures show that the cylinder pressure-crank angle, cylinder temperature-crank angle, and heat release rate-crank angle (HRR-CA) diagrams are fairly similar to each other and follow the typical behaviour of NDF under different operating conditions. Here, the HRR has been determined by averaging over 100 consecutive cycles for NDF and five different WRs with CA under full load at five selected different engine speeds. The effects of WAIA on the CDs, which were determined from HRR, were investigated and shown in Figures 7 (a-e).

a) 2000 rpm: The effects of WAIA on the cylinder pressure, temperature, and HRR at 2000 rpm are shown in Figures 2 (a-b-c), respectively. Also, the effects of WAIA on the CD are shown in Figure 7 (a). As can be seen in Figure 2(a), the WAIA cylinder pressure profiles are similar to NDF and the effects of water addition on cylinder pressure seem insignificant. For example, at this engine speed, for NDF the peak cylinder pressure is 156.57 bar and it occurs at 11.15 °CA, while for (2.415, 4.215, 5.945, 8.321, and 9.462) % WRs the peak cylinder pressures become (158.16, 157.05, 156.81, 158.25, and 156.96) bar, respectively and they take place at (10.68, 10.54, 10.72, 10.70, and 11.05) °CA, respectively. The maximum cylinder pressure values for the selected five WRs are slightly higher than that of NDF and the peak cylinder pressure angles occur earlier than that of NDF. This can be attributed to a longer ignition delay because of the cooling effect of water on the inlet air temperature. This observation agrees with the relevant literature (Subramanian, 2011; Tesfa et al., 2012; Gowrishankar and Krishnasamy, 2022; Abu-Zaid, 2004).

As can be seen in Figure 2 (b), WAIA decreases cylinder temperatures. For NDF the peak cylinder temperature is 2168.03 K and it occurs at 21.09 °CA, while for (2.415, 4.215, 5.945, 8.321, and 9.462) % WRs the peak cylinder temperature values become (2055.32, 2039.91, 2052.84, 2068.79 and 2028.79) K, respectively and they take place at (21.513, 21.690, 21.188, 21.850 and 21.283) °CA, respectively. With WAIA, the cylinder temperature values during the compression process will be lower than NDF as water that is injected into intake air will vaporize and cools the air. This will also result in a reduction in combustion temperature. As it is known from the literature that applying the water adding method in engines decreases cylinder temperature values which is naturally an expected result (Subramanian, 2011; Şahin et al., 2014; Ithnin et al., 2015). In addition, the effect of water on cylinder temperature is explained in reference Zhao et al. (2018), as follows: When WAIA method is applied, the liquid water could evaporate in the cylinder during the intake and compression phases. Thus, the cylinder temperature drops since the latent heat of the evaporation of water is larger (Zhao et al., 2018).

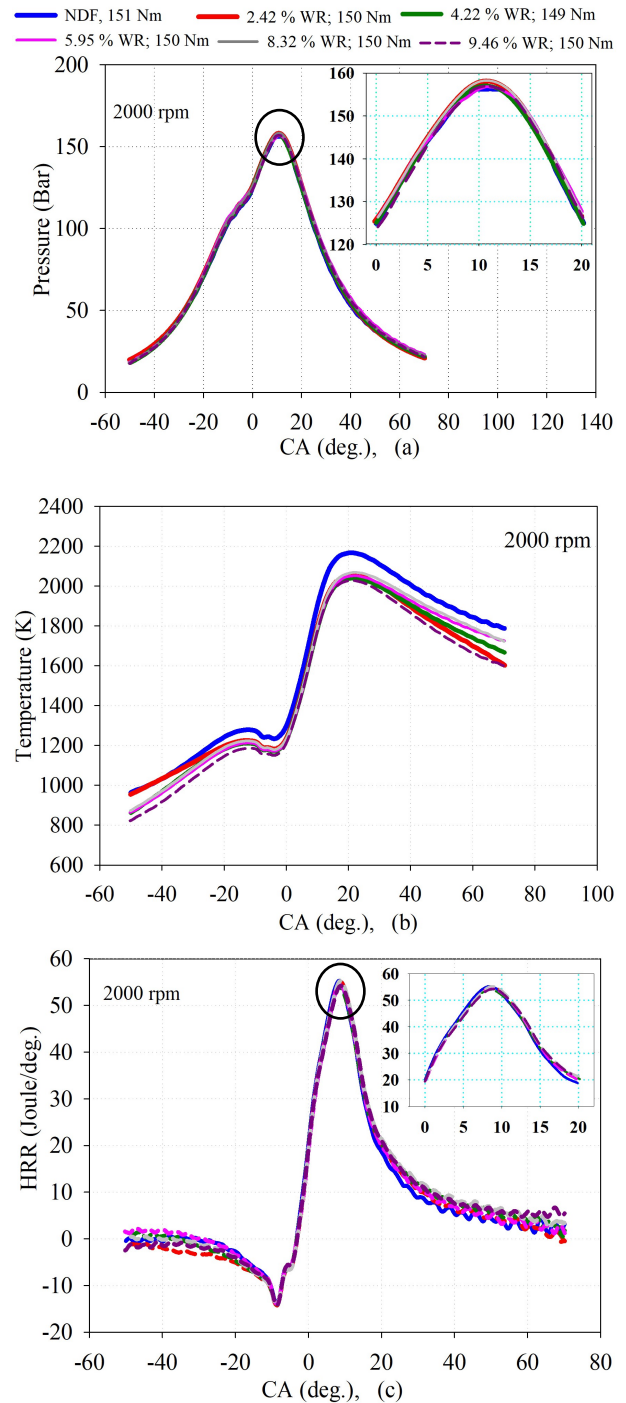
Figure 2 (c) shows the variations of HRR for NDF and five different WRs under full load. As can be seen in this figure, HRR values with WAIA are lower than that of NDF at the beginning of the combustion, around of the TDC. However, they have increased toward the end of the combustion process. Similar results have been obtained in the literature (Subramanian, 2011; Zhang et al., 2017; Vigneswaran et al., 2021). For NDF, the maximum value of HRR is 55.27 J/deg. and it occurs at 8.44 °CA, while for (2.415, 4.215, 5.945, 8.321, and 9.462) % WRs the maximum values of HRR become (55.01, 53.96, 54.39, 55.22, and 54.20) J/deg. respectively and they take place at (8.88, 8.45, 8.60, 8.89, and 8.77) °CA, respectively. We could see in Figure 2 (c) that, the maximum values of the HRR for all selected WRs are lower than that of NDF and the maximum HRR angles occur later than that of NDF. With the WAIA, we

can say that the combustion starts a little later and the combustion might continue during the expansion stroke. However, combustion has been completed earlier with water addition. This can be observed from the CD values given below: For example, using the HRR values, the CDs are also determined and 10 %–90 % of the maximum heat release rate was used as the CD (Park and Oh, 2022; Gentz et al., 2015; Hosseini and Checkel, 2006). As can be seen in Figure 7(a), WAIA has decreased CDs at 2000 rpm generally. For NDF, the CD is 13.10 °CA, while for (2.415, 4.215, 5.945, 8.321, and 9.462) % WRs the CD values become (12.96, 12.93, 12.68, 12.95, and 13.576) °CA respectively.

Thus, with the shortening of the CD, approximately the same amount of fuel is burned closer to TDC, which shows the enhancing effect of WAIA on combustion. The burn of the fuel around TDC without forming knocking has a useful effect on reducing of fuel consumption (Heywood, 1988). BSFC decreases at 2000 rpm at low loads, and the maximum decrease rate obtained in BSFC was 2.68% for approximately 6% water under 120 Nm load (Şahin et al., 2018; Şahin et al., 2014; Tuti et al., 2021). Also, it can be thought that the homogeneous combustion, which might be occurred by WAIA, causes the burning process of the fuel to be accelerated, which decrease CD. Similar explanations and results have been given in the literature (Zhang et al., 2017; Park and Oh, 2022).

b) 2500 rpm: The effects of WAIA on the cylinder pressure, temperature, and HRR at 2500 rpm are presented in Figures 3 (a-b-c), respectively. Also, the effects of WAIA on the CD are shown in Figure 7 (b). As can be seen in Figure 3(a); for NDF the peak cylinder pressure is 164.08 bar and it occurs at 9.94 °CA, while for (1.889, 4.215, 6.192, 8.551, and 9.687) % WRs the peak cylinder pressure values become (164.101, 164.088, 164.99, 164.29, and 164.38) bar, respectively and they take place at (9.77, 9.58, 9.77, 9.76, and 9.75) °CA, respectively. The maximum cylinder pressure values for the selected five WRs are higher than that of NDF and the peak cylinder pressure angles occur earlier than that of NDF. As dictated above, it is thought that higher cylinder pressure values with WAIA occurred due to the increased ignition delay. In fact, the water addition has a restricted effect on the cylinder pressure as 2000 rpm.

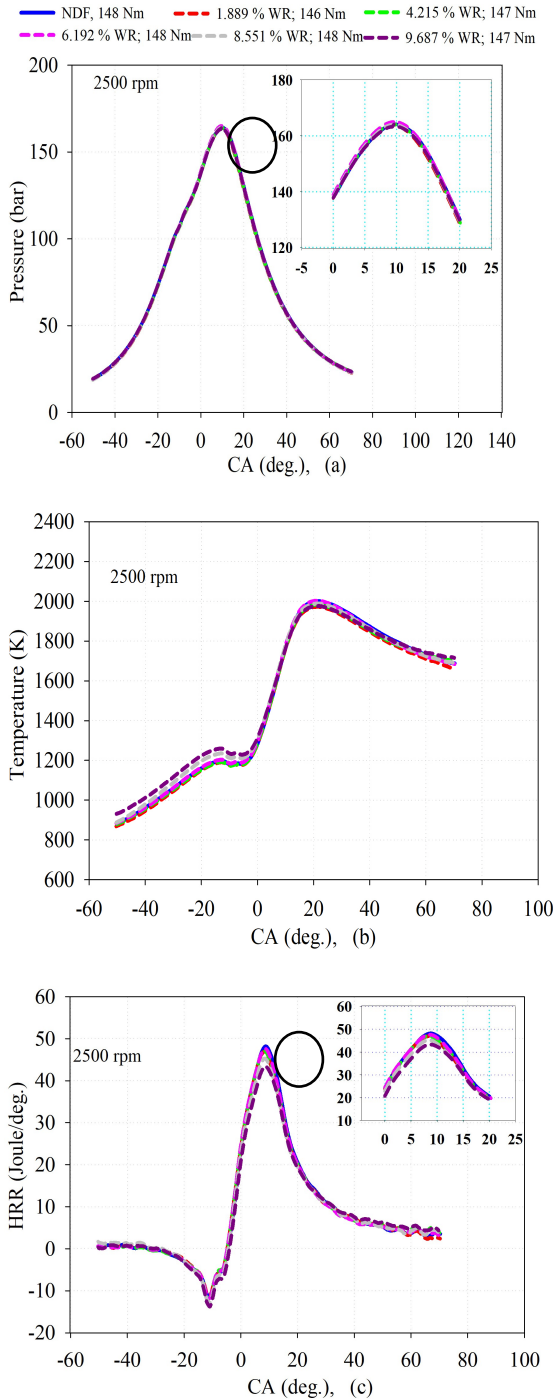
As can be seen in Figure 3 (b), WAIA decreases cylinder temperature values. For NDF the peak cylinder temperature is 2000.74 K and it occurs at 21.57 °CA, while for (1.889, 4.215, 6.192, 8.551, and 9.687) % WRs the peak cylinder temperature values become (1972.86, 1984.01, 2002.86, 1988.47, and 1976.19) K, and they take place at (21.42, 21.22, 21.79, 21.40, and 21.75) °CA, respectively. Thus, it can be said that WAIA decreases cylinder temperature values generally. It is known from the literature that added water may absorb the heat of vaporization during compression and combustion processes, and this reduces the cylinder temperature values (Subramanian, 2011; Zhang et al., 2017; Park and Oh, 2022).



Figures 2 (a-b-c). Cylinder pressure, cylinder temperature and HRR variations for different WRs in respect to CA at 2000 rpm, respectively.

As can be seen in Figure 3 (c), HRR values with WAIA are lower than that of NDF at the beginning of the combustion, around TDC. After that, as combustion was advanced, HRR characteristics followed nearly that of NDF, and HRR values have been very close to NDF. At 2500 rpm, it could be observed that the combustion process with WAIA has not actually improved as expected. Thus, WAIA increases BSFC somewhat at this engine speed. For example, the increase ratios of BSFC for (2.065, 4.013, 6.196, 8.261, and 9.400) % WRs under 149 Nm full load have been (1.088, 2.177, 1.630, 0., and

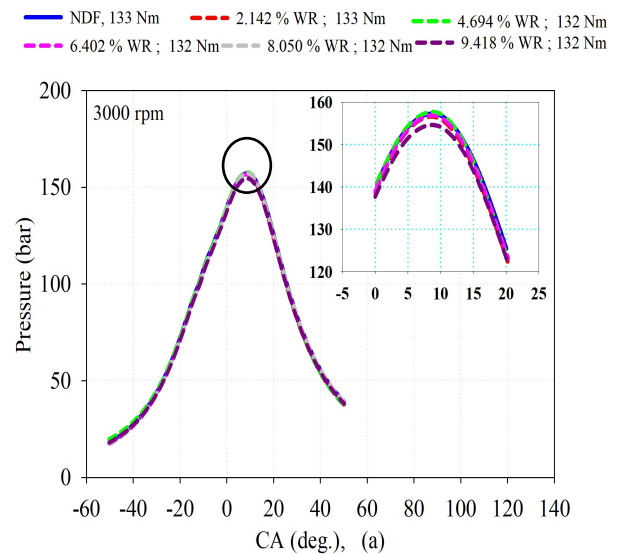
2.719)% respectively. Similar results have been found under low loads. For NDF, the maximum value of HRR is 48.21 J/deg. and it occurs at 8.82 °CA, while for (1.889, 4.215, 6.192, 8.551, and 9.687) % WRs the maximum values of HRR become (46.96, 47.13, 47.64, 45.31, and 43.33) J/deg. respectively and they take place at (8.27, 8.45, 8.64, 8.26, and 8.63) °CA, respectively. As can be seen in Figure 7 (b), for NDF, the CD is 15.19

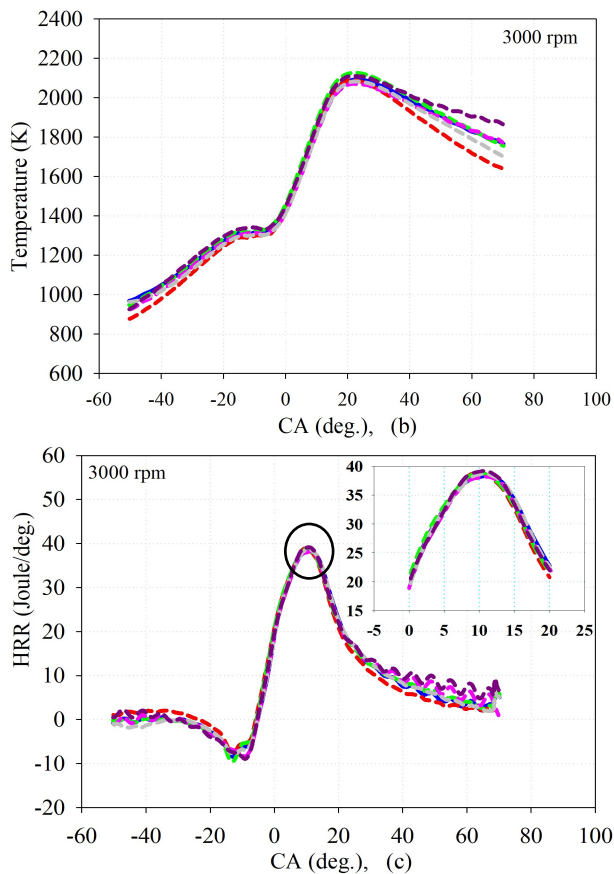


Figures 3 (a-b-c). Cylinder pressure, cylinder temperature and HRR variations for different WRs in respect to CA at 2500 rpm, respectively. °CA, while for (1.889, 4.215, 6.192, 8.551, and 9.687) % WRs the CDs are (14.66, 14.17, 14.04, 14.35, and 14.62) °CA respectively. Thus, it can be said that WAIA has decreased slightly CDs at 2500 rpm.

c) 3000 rpm: The effects of WAIA on the cylinder pressure, temperature, HRR, and CD at 3000 rpm are shown in Figures 4 (a-b-c) and Figure 7 (c), respectively. As can be seen in Figure 4 (a) for NDF the peak cylinder pressure is 155.99 bar and it occurs at 8.35 °CA, while for (2.142, 4.694, 6.402, 8.050, and 9.418) % WRs the peak cylinder pressure values become (154.45, 157.55, 154.57, 155.11 and 156.92) bar, respectively and they take place at (8.78, 8.35, 8.56, 8.34 and 8.34) °CA, respectively. Thus; cylinder pressure values increase for 4.694% and 9.418% WRs and they decrease for other WRs. However, the peak cylinder pressure values show only minor differences in magnitude for selected operating conditions at this engine speed.

As can be seen in Figure 4 (b), WAIA decreases cylinder temperature values. For NDF the peak cylinder temperature is 2091.44 K and it occurs at 22.34 °CA, while for (2.142, 4.694, 6.402, 8.050, and 9.418) % WRs the peak cylinder temperature values become (2089.40, 2126.81, 2070.62, 2083.20, and 2110.92) K, respectively and they take place at (21.38, 22.34, 21.63, 22.32, and 21.86) °CA, respectively. Thus, peak cylinder temperature values generally decrease. Whereas for (4.694 and 9.418) % WRs, cylinder temperature values increase. As can be seen from the evaluation of the heat analysis graphs below, the maximum values of HRR at this engine speed are generally higher and occur closer to the TDC than that of NDF. Thus, it could be said that combustion takes place closer to the TDC and occurs faster especially for (4.694 and 9.418) % WRs, which may result in increased cylinder temperature values. As shown in Figure 7 (c), the lowest CD has taken place for 4.694% WR at approximately 2.37% reduction level. Hence, the highest combustion temperature increment has reached approximately 1.69% approximately, for this WR.





Figures 4 (a-b-c). Cylinder pressure, cylinder temperature and HRR variations for different WRs in respect to CA at 3000 rpm, respectively.

As can be seen in Figure 4 (c), HRR values with WAIA are slightly higher than that of NDF at the beginning of the combustion, around the TDC. After that, as combustion was advanced during the expansion stroke, HRR values become slightly higher than that of NDF. For NDF, the maximum values of HRR are 38.27 J/deg. and it occurs at 11.06 °CA, while for (2.142, 4.694, 6.402, 8.050, and 9.418) % WRs the maximum values of HRR become (38.95, 38.79, 38.17, 38.70, and 39.19) J/deg. respectively, and they take place at (9.68, 9.71, 10.81, 10.60, and 10.60) °CA, respectively. It has been observed from this experimental data that the maximum values of HRR for selected WRs become generally higher than that of NDF, and the burning of the diesel fuel takes place closer to the TDC. For NDF, the CD is 18.96 °CA, while for (2.142, 4.694, 6.402, 8.050, and 9.418) % WRs the CD values become (18.69, 18.51, 18.42, 18.66, and 18.71) °CA respectively, as can be seen in Figure 7 (c). WAIA has decreased CDs slightly at 3000 rpm. It is thought that this reduction takes place due to the improvement of combustion because of the formation of a more homogeneous and faster fuel-air mixture with the water addition.

d) 3500 rpm: The effects of WAIA on the cylinder pressure, cylinder temperature, HRR, and CD at 3500 rpm are shown in Figures 5 (a-b-c) and Figure 7 (d), respectively. As can be seen in Figure 5(a); for NDF the

peak cylinder pressure is 158.16 bar, and it occurs at 6.82 °CA, while for (2.142, 3.689, 6.402, 8.050, and 12.245) % WRs the peak cylinder pressure values become (158.75, 158.05, 159.28, 159.65, and 159.54) bar, and they take place at (6.31, 6.84, 6.56, 6.56, and 6.82) °CA, respectively. The maximum cylinder pressure values for selected WRs are higher than that of NDF, and the peak cylinder pressure values occur earlier than that of NDF. In other words, combustion took place in a shorter time with WAIA, as can be seen in Figure 7 (d). The reasons for this increase in cylinder pressure for this engine speed are almost similar to the other selected engine speeds as explained above. In fact, at this speed, the effect of water addition on cylinder pressure has become at a low level as the increase values of cylinder pressures are under 1 %.

As can be seen in Figure 5 (b), WAIA increases slightly cylinder temperature values. For NDF the peak cylinder temperature is 2048.08 K, and it occurs at 22.04 °CA, while for (2.142, 3.689, 6.402, 8.050, and 12.245) % WRs the peak cylinder temperature values become (2048.19, 2026.37, 2051.18, 2056.11, and 2053.64) K, respectively and they take place at (22.07, 22.10, 21.79, 21.79, and 21.51) °CA, respectively. It could be observed from this data that the cylinder temperature values increased in general with WAIA at 3500 rpm. The possible reason for this temperature increment might be the burning of the injected diesel fuel in a shorter time.

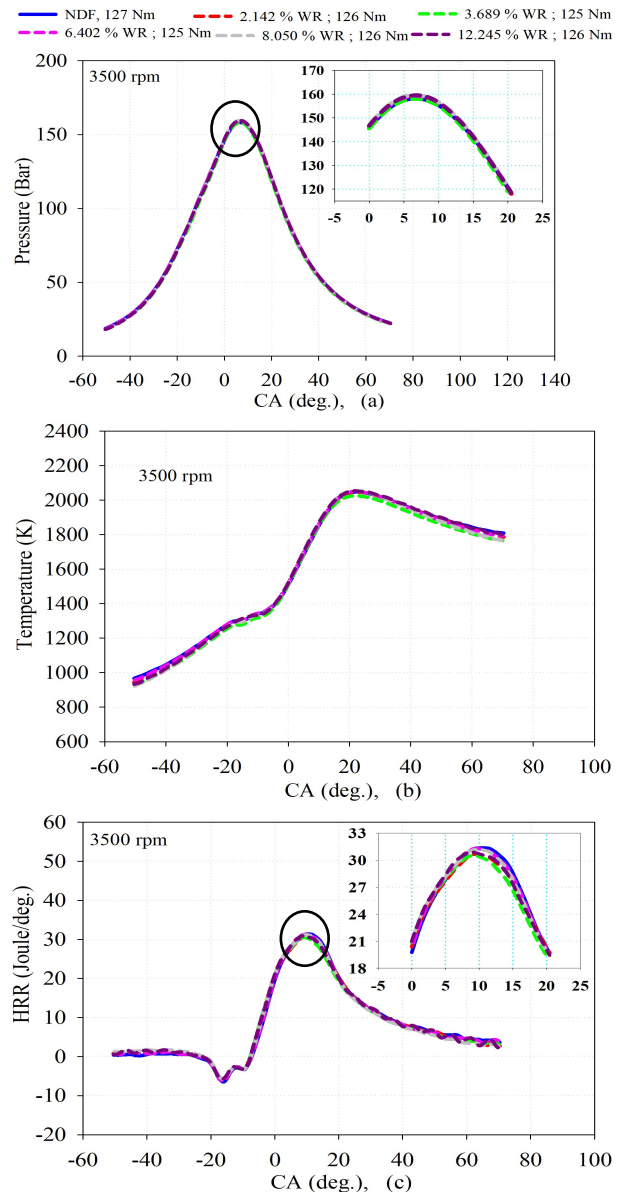
In Figure 5(c), the variations of HRR have been indicated for NDF and five different WRs under full load. As can be seen in this figure, HRR values with WAIA take lower values than that of NDF at the beginning of the combustion, around the TDC. However, they have increased towards the end of the combustion process. For NDF, the maximum value of HRR is 31.38 J/deg., and it occurs at 10.50 °CA, while for (2.142, 3.689, 6.402, 8.050, and 12.245) % WRs the maximum values of HRR become (30.65, 30.52, 31.29, 31.17, and 30.91) J/deg. and they take place at (9.46, 9.47, 9.72, 9.72, and 8.92) °CA, respectively. We can notice in Figure 5(c), the maximum values of the HRR for all of the selected WRs are lower than that of NDF and the maximum HRR values occur at smaller crank angles than that of NDF. For NDF, the CD is 21.51 °CA, while for (2.142, 3.689, 6.402, 8.050, and 12.245) % WRs the CD values become (21.28, 20.93, 20.72, 21.01, and 21.31) °CA respectively. Here, the maximum decrement ratio of the CD was at the level of rate 3.67 % at 6.402 % WR. The reduction in HRR was also low at the level of 0.03 % for this WR. Thus, it can be advised to apply this WR at 3500 rpm.

e) 4000 rpm: The effects of WAIA on the cylinder pressure, temperature, HRR, and CD at 3000 rpm are shown in Figures. 6 (a-b-c) and Figure 7 (e), respectively. As can be seen in Figure 6 (a) for NDF the peak pressure is 157.99 bar and it occurs at 5.42 °CA, while for (1.860, 4.467, 5.705, 8.321, and 9.236) % WRs the peak cylinder pressure values become (153.68, 153.04, 154.74, 157.22 and 156.05) bar, and they take place at (5.42, 6.05, 5.42, 4.85, and 5.72) °CA, respectively. As can be seen in

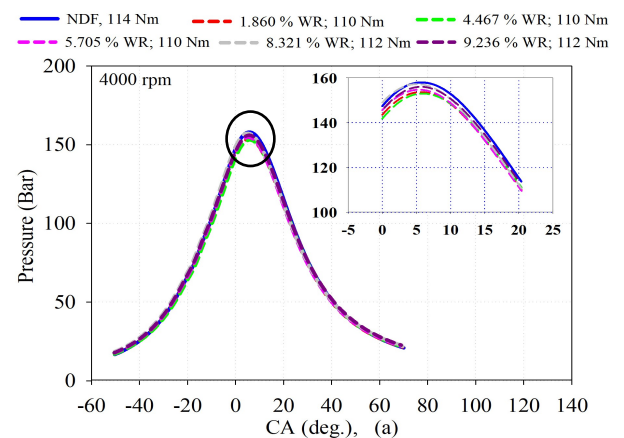
Figure 6 (a), the maximum cylinder pressure values are lower than NDF for all of the selected WRs and they occur earlier than that of NDF. Contrary to the other engine speeds, cylinder pressures have decreased at 4000 rpm, which is the nominal speed of this engine. It is well known that automotive diesel engines run in a very short time at this engine speed in practice application. In the literature; Subramanian (2011) also stated that the usage of water in diesel engines reduces the maximum cylinder pressure. Ayhan and Ece (2020) have studied the effect of electronically controlled direct water injection into the cylinder at compression stroke on engine performance, combustion, and exhaust emissions, and they found that water injection decreases cylinder pressure at 2200 rpm, which was the nominal engine speed of their engine.

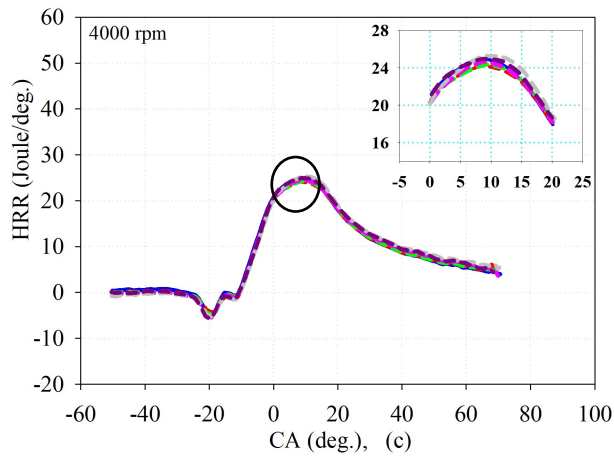
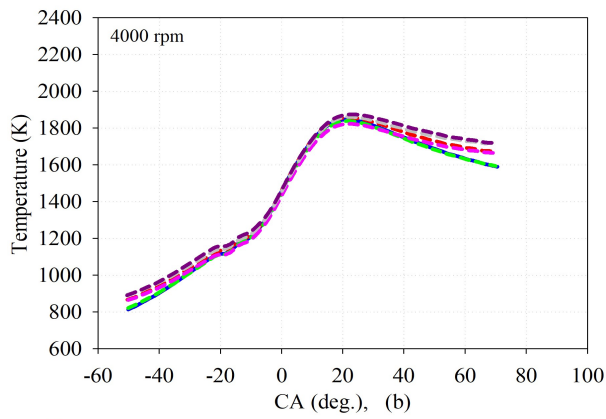
As can be seen in Figure 6 (b), WAIA generally decreases cylinder temperature values. For NDF the peak temperature is 1846.58 K and it occurs at 21.32 °CA, while for (1.860, 4.467, 5.705, 8.321, and 9.236) % WRs the cylinder peak temperature values become (1857.42, 1838.21, 1823.01, 1861.15, and 1874.60) K, and they take place at (21.60, 21.32, 22.59, 21.64, and 23.01) °CA, respectively. Peak cylinder temperature values increase for (1.860, 8.321, and 9.236) % WRs but they decrease for (4,467 and 5,705) % WRs. It has been observed in Figures 6 (a and b) and during the experiments that the cylinder temperature and the pressure variations are not quite consistent at 4000 rpm. As mentioned above, this speed is a very little used engine speed under the normal operating period of automotive diesel engines, and the running of the engine is not stable.

In Figure 6 (c), the variations of HRR have been shown for NDF and five different WRs under full load. As can be seen in these figures HRR values with WAIA are close to that of NDF generally and lower at the beginning of the combustion, around TDC. After that, as combustion was advanced, HRR curves followed nearly NDF characteristics, and HRR values have been almost equal to NDF values. For NDF, the maximum values of HRR are 24.98 J/deg. and it occurs at 8.71 °CA, while for (2.142, 3.689, 6.402, 8.050, and 12.245) % WRs the maximum values of HRR become (24.21, 24.35, 24.64, 25.29, and 24.94) J/deg. respectively, and they take place at (9.00, 9.31, 8.71, 9.02, and 8.66) °CA, respectively. Here, it could be observed that the maximum values of the HRR in all selected WRs were generally lower than that of NDF. It could be also seen from these curves that the combustion process could not be improved with the application of WAIA as expected, for 4000 rpm. For NDF, the CD is 24.32 °CA, while for (1.860, 4.467, 4.467, 5.705, 8.321, and 9.236) % WRs the CDs become (24.25, 24.12, 24.02, 26.44, and 28.88) °CA. For (1.860, 4.467, and 5.705)% WRs, the decrease ratios in the CD values are (0.28, 0.81, and 1.23) %, but for (8.321 and 9.236) % WRs, the increase ratios in the CD values become (8.73 and 18.76) %, respectively. In fact, the variation ratios in CD are at low levels and they take place within the error limits.



Figures 5 (a-b-c). Clinder pressure, cylinder temperature and HRR variations for different WRs in respect to CA at 3500 rpm, respectively



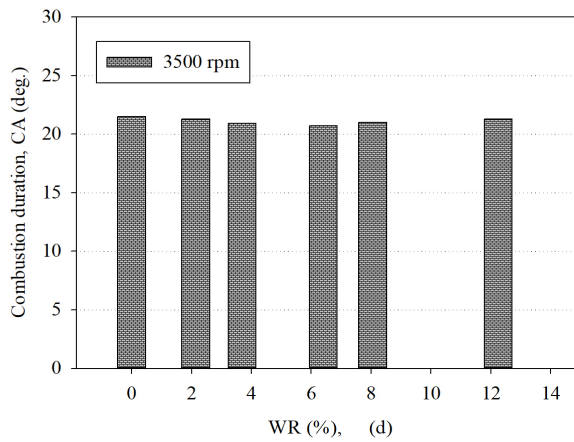
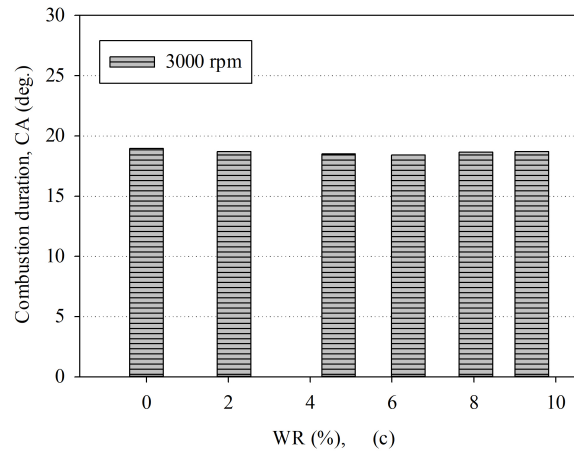
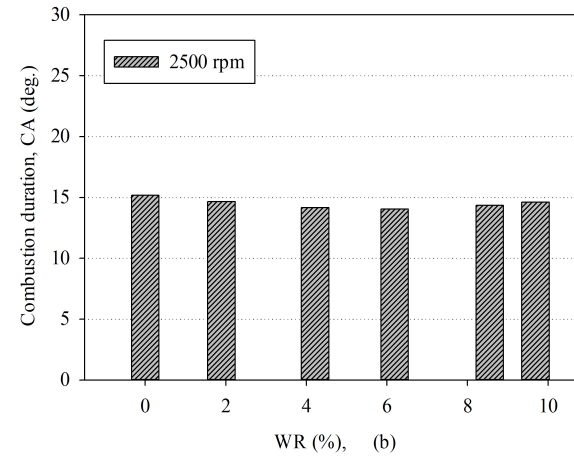
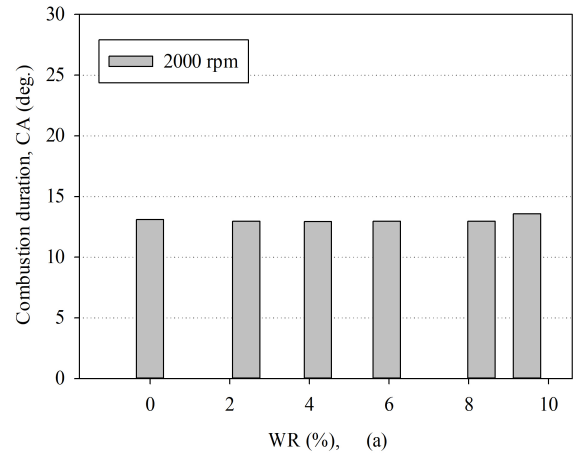


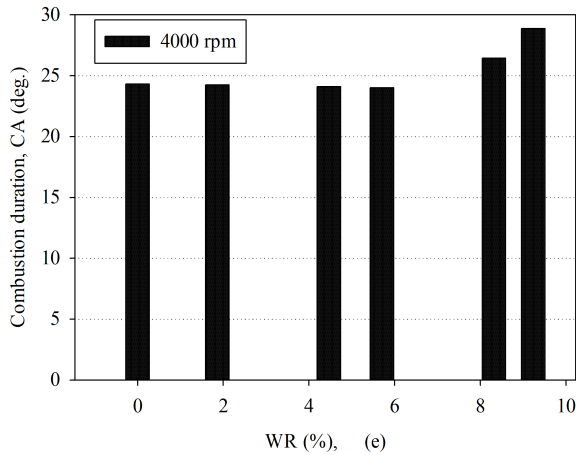
Figures 6 (a-b-c). Cylinder pressure, cylinder temperature and HRR variations for different WRs in respect to CA at 4000 rpm, respectively.

Here; using the developed empirical correlation, CDs were also calculated for NDF and (2.5, 5, and 7.5) % WRs at 2250 rpm, (80, 70, and 60) Nm load conditions, which were not tested, and the calculated values are presented in Table 9. As a result, we can say that by using the developed empirical correlation, the CD can be determined at any desired condition for this engine. Also, this correlation can be used for different diesel engines, and it could give useful information for the combustion duration of these engines. As can be seen from Table 9, the CDs are decreased with the WR in all of the selected operating conditions.

Table 9. Computed CD by using the developed empirical correlation for three WRs under three load at 2250 rpm.

WR (%)	2250 rpm		
	80 Nm	70 Nm	60 Nm
	CD (°CA)	CD (°CA)	CD (°CA)
NDF	22.799	22.778	22.111
2.5	22.651	22.670	22.071
5	22.590	22.609	22.012
7.5	22.617	22.595	21.933





Figures 7 (a-b-c-d-e). CD variations for different WRs at 2000, 2500, 3000, 3500, and 4000 rpms under full load, respectively.

The Effects of WAIA on Energy Balance

In this section, the effects of WAIA on the energy balance analysis are presented in Figures 8 at 2000 and 4000 rpms under only full load conditions. Here, the energy balance evaluations were made according to the fuel chemical energy. As can be seen in Figure 8 (a), the effective power values according to the chemical energy of the fuel generally decrease with WAIA at 2000 rpm. The effective power values according to fuel chemical energy for NDF and (2.419, 4.215, 5.945, 8.321, and 9.482) % WRs have become 34.707 and (33.969, 34.253, 34.769, 34.344, and 34.189) respectively. Here, it could be observed that the effective power values according to fuel chemical energy in all selected WRs were generally lower than that of NDF. For only 5.945 % WR, this value is higher than that of NDF. Exhaust losses generally decrease with WAIA. As can be seen from Figure 2(b) given above, the cylinder temperatures and also exhaust temperatures decrease with the addition of water, which reduces exhaust losses. However, the exhaust losses increase for 9.462 % WR. The combustion continues in the expansion process because of the increase in burning duration with this water ratio.

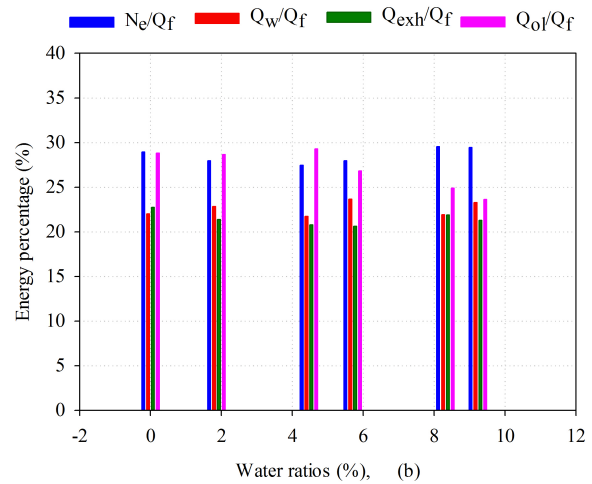
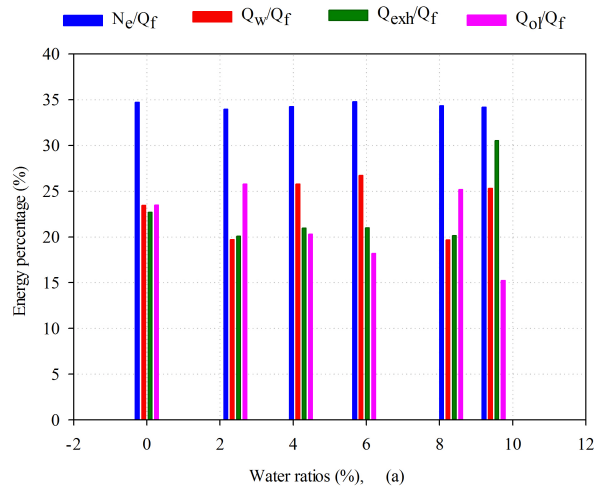


Figure 8. The energy balance of the used test engine for different WRs under full load condition, (a) 2000 rpm, and (b) 4000 rpm, respectively

For this reason, the exhaust temperature may be slightly higher, increasing the exhaust losses. The heat losses to cooling water generally tend to increase with the addition of water although the change of these values is not very smooth. The other losses are generally reduced with the WAIA.

The influence of the WAIA on the energy balance at 4000 rpm is shown in Figure 8b. It can be seen from this figure that the effective power values according to the chemical energy of the fuel decrease until 8.32 % WR but, after this ratio, these values slightly start to increase at 4000 rpm. Similarly, CDs and the values of HRR increase for (8.321 and 9.236) % WRs. The addition of water into the intake air between approximately (6-10) percent is thought to improve combustion at 4000 rpm, which increases effective power from the interpretation of these results. The water addition to the intake air slightly reduces the exhaust losses but, it increases the heat losses to cooling water at this engine speed according to the chemical energy of the fuel. Although the exhaust temperature slightly increased with the addition of water at 4000 rpm, the exhaust losses decrease according to the added fuel energy. The reason for this is that the injected fuel mass is more with the addition of water at this engine speed. With the water addition into intake air at 4000 rpm, the air in the intake channel also cools well because of the evaporation of water. This can increase the volumetric efficiency of the engine. This explanation agrees with the literature (Zhanming et al., 2022; Subramanian, 2011). Thus, depending on the electronic control unit, more fuel may be injected. In fact, the change in exhaust losses according to fuel chemical energy is not very high with a minimum value of 21.74% and a maximum value of 22.74%. WAIA generally decreases the other losses. The other losses are generally reduced with the water addition into the intake.

CONCLUSION

In the present study, the effects of water addition into intake air on the cylinder pressure, cylinder temperature, HRR, and CD were experimentally investigated and compared with NDF in an automotive diesel engine. Based on the experimental results, the main obtained results can be summarized as follows:

1. Cylinder pressure values generally increased at (2000, 2500, and 3500) rpms, but they decreased at (3000 and 4000) rpms for all of the selected WRs. The crank angles in which the maximum cylinder pressure values occurred have been closer to TDC with WAIA.

2. Cylinder temperature values mostly decreased at (2000, 2500, and 3000) rpms, but they generally increased at (3500, and 4000) rpms for WAIA. Also; maximum cylinder temperature values occurred at crank angles farther from TDC with WAIA.

3. The characteristic behaviour of the HRR-crank angle curve for water adding has been very similar to that of the NDF at all of the selected engine speeds. HRR values generally decreased at (2000, 2500, 3500, and 4000) rpms, but generally increased at 3000 rpm.

4. The CD values were generally shortened at all of the engine speeds under full loads with water addition. CD values for NDF and for (2.42, 4.22, 5.95, 8.32, and 9.46) % WRs have been determined as (13.10, 12.96, 12.93, 12.68, 12.95, and 13.576) °CA respectively at 2000 rpm.

5. Using the HRR curves, an empirical correlation has been developed for estimating the CD for the test engine. This quadratic relation has been developed by applying the multiple least squares curve fitting method, considering experimental results for different WRs, different engine loads and different engine speeds. By using this empirical formula CD at any condition can be estimated for this test engine. Similar correlations can be performed for different diesel engines, and this way, generalised results can be obtained.

Using the developed empirical relation, the CD can be estimated for any operation condition which is different from the experiments. For example; at 2250 rpm under 80 Nm load condition, CDs have been determined as (22.80, 22.65, 22.59, and 22.62) °CA for NDF and WRs of (2.5, 5, 7.5) %.

6. The effective power values according to the chemical energy of the fuel generally decrease with WAIA at 2000 rpm. However, the effective power values according to the chemical energy of the fuel generally decrease until 8.32 % WR but, after this ratio, these values slightly start to increase at 4000 rpm. WAIA decreases generally the exhaust losses at 2000 rpm, but it increases the exhaust losses at 4000 rpm. The heat losses to cooling water generally tend to increase with the water addition into the intake air.

REFERENCES

Abu-Zaid M., 2004, Performance of single cylinder, direct injection diesel engine using water fuel emulsions, *Energy Conv. and Management*, 45, 697-705.

Ayhan V. and Ece Y.M., 2020, New application to reduce NO_x emissions of diesel engines: Electronically controlled direct water injection at compression stroke, *Applied Energy*, 260, 114328.

Boldaji R.M. and Sofianopoulos A., Mamalis S., Lawler B., 2018, Effects of mass, pressure, and timing of injection on the efficiency and emissions characteristics of TSCI combustion with direct water injection, *SAE Technical Papers*, 2018-01-0178.

Durgun O. and Kafali K., 1991, Blockage correction, *Ocean Engineering*, 18, 2699-82.

Elsanusi O.A., Roy M.M. and Sidhu M.S., 2017, Experimental invest. on a diesel engine fueled by diesel-biodiesel blends and their emulsions at various engine operating conditions, *Applied Energy*, 203, 582–93.

El Shenawy E.A., Elkelawy M., Mohamood H.A.E, Shams M.H., Panchal H. and Sadasivuni K.K., 2019, Investigation and performance analysis of water-diesel emulsion for improvement of performance and emission characteristics of partially premixed charge compression ignition (PPCCI) diesel engines, *Sustainable Energy Technologies and Assessments*, 36, 100546.

Ghazal O.H., 2019, Combustion analysis of hydrogen-diesel dual fuel engine with water injection technique, *Case Studies in Thermal Engineering*, 13, 100380.

Gentz G., Thelen B., Litke P., Hoke J. and Toulson E., 2015, Combustion visualization, performance, and CFD modeling of a pre-chamber turbulent jet ignition system in a rapid comp. machine, *SAE Int J Engines*, 8, 538–46.

Gowrishankar S. and Krishnasamy A., 2022, A relative assessment of emulsification and water injection methods to mitigate higher oxides of nitrogen emissions from biodiesel fueled light-duty diesel engine, *Fuel*, 308, 121926.

Gowrishankar S., Rastogi P. and Krishnasamy A., 2020, Investigations on NO_x and smoke emissions reduction potential through water-in-diesel emulsion and water fumigation in a small-bore diesel engine, *SAE Technical Paper*, 2020-32-2312.

Han J., Somers L.M.T., Cracknell R., Joedicke A., Wardle R. and Mohan V.R.R., 2020 Experimental investigation of ethanol/diesel dual -fuel combustion in a heavy -duty diesel engine, *Fuel*, 275, 117867.

Heywood J.B., 2018, Internal Combustion Engine Fundamentals (2nd edit), McGraw-Hill Book Company.

Hosseini V. and Checkel M.D., 2006, Using reformer gas to enhance HCCI combustion of CNG in a CFR engine, *SAE Technical Paper*, 01, 13.

- Ithnin A.M., Ahmad M.A., Bakar M.A.A., Rajoo S. and Yahya W.J., 2015, Combustion performance and emission analysis of diesel engine fuelled with water-in-diesel emulsion fuel made from low-grade diesel fuel, *Energy Conv. and Management*, 90, 375–82.
- Jhalani A., Sharma D., Soni S.L. and Sharma P.K., 2019, Effects of process parameters on performance and emissions of a water-emulsified diesel-fueled compression ignition engine, *Energy Sources, Part A: Recovery, Utilization, and Environmental Effects*, 1–13.
- Khanjani A. and Sobati M.A., 2021, Performance and emission of a diesel engine using different water/waste fish oil (WFO) biodiesel/diesel emulsion fuels: Optimization of fuel formulation via response surface methodology (RSM), *Fuel*, 288, 119662.
- Maawa W. N., Mamat R., Najafi G. and Goey LPH. D., 2020, Performance, comb., and emission characteristics of a CI engine fueled with emulsified diesel-biodiesel blends at different water contents, *Fuel*, 267, 117265.
- Mahmood A.S., Qatta H.I., Hussein N.F. and Ismael A.A., 2019, Effect of using diesel-water emulsion as a fuel on diesel engine emissions: An experimental study. *International Journal of Energy and Environ.*, 10, 321-8.
- Park J. and Oh J., 2022, Study on the characteristics of performance, comb., and emissions for a diesel water emulsion fuel on a combustion visualization engine and a commercial diesel engine, *Fuel*, 311, 122520.
- Singh S.B., Dhar A. and Agarwal A.K., 2015, Technical feasibility study of butanol-gasoline blends for powering medium-duty transportation spark ignition engine, *Renewable Energy*, 76, 706-716.
- Shojaei T.R., Khalife E., Tabatabaei M., Najafi B. and Mirsalim M., 2019, Effect of nano-cerium oxide and water additives on B5 combustion emissions, *Zanco Journal of Pure and Applied Sciences*, 31, 34–9.
- Subramanian K.A., 2011, A comparison of water–diesel emulsion and timed injection of water into the intake manifold of a diesel engine for simultaneous control of NO and smoke, *Energy Conv. & Mana.*, 52, 849–57.
- Sun X., Ning J., Liang X., Jing G., Chen Y. and Chen G., 2022, Effect of direct water inj. on comb. and emissions charact. of marine diesel engines, *Fuel*, 309, 122213.
- Şahin Z., Tuti M. and Durgun O., 2014, Experimental investigation of the effects of water adding to the intake air on the engine performance and exhaust emissions in a DI automotive diesel engine, *Fuel*, 115, 884–895.
- Şahin Z., Durgun O. and Tuti M., 2018, An experimental study on the effects of inlet water injection of diesel engine heat release rate, fuel consumption, opacity, and NO_x emissions, *Exergetic, Energetic and Environmental Dimensions*, 981-96.
- Tauzia X., Maiboom A. and Shah SR., 2010, Experimental study of inlet manifold water injection on combustion and emissions of an automotive direct injection diesel engine. *Energy*, 35, 3628–39.
- Tesfa B., Mishra R., Gu F. and Ball A.D., 2012, Water injection effects on the performance and emission characteristics of a CI engine operating with biodiesel, *Renewable Energy*, 37, 1, 333-344.
- Tuti M., Şahin Z. and Durgun O., 2021, Experimental investigation of the effects of water addition into the intake air on cylinder pressure, temperature, heat release rate and combustion duration in an automotive diesel engine, *23rd Congree on Thermal Science and Technology*, September 8-10, Gaziantep, Türkiye, 785–95.
- Vigneswaran R., Balasubramanian D. and Sastha B.D.S., 2021, Performance, emission and combustion characteristics of unmodified diesel engine with titanium dioxide (TiO₂) nano particle along with water-in-diesel emulsion fuel, *Fuel*, 285, 119115.
- Zhang Z., Kang Z., Jiang L., Chao Y., Deng J., Hu Z., Li L. and Wu Z., 2017, Effect of direct water injection during compression stroke on thermal efficiency optimization of common rail diesel engine, *Energy Procedia*, 142, 1251-1258.
- Zhanming C., Long W., Xiaochen W., Hao C., Limin G. and Nan G., 2022, Experimental study on the effect of water port injection on the combustion and emission characteristics of diesel/methane dual-fuel engines, *Fuel*, 312, 122950.
- Zhao R., Zhang Z., Zhuge W., Zhang Y. and Yin Y., 2018, Comparative study on different water/steam injection layouts for fuel reduction in a turbocompound diesel engine, *Energy Conv. & Manag.*, 171, 1487-501.
- Zhu S., Hu B., Akehurst S., Copeland C., Lewis A. and Yuan H., 2019, A review of water injection applied on the internal combustion engine, *Energy Conv. & Management*, 184, 139–158.